7

Electromotive Force Measurements in High-Temperature Systems

Dominika Jendrzejczyk-Handzlik and Krzysztof Fitzner
AGH University of Science and Technology, Laboratory of Physical Chemistry and Electrochemistry, Faculty of Non-Ferrous Metals, Krakow, Poland

1. Introduction

Stability of phases existing in chemical systems is determined by its Gibbs free energy designated as G. The relative position of Gibbs free energy surfaces in the G–T–X (composition) space determines stability ranges of respective phases yielding a map called the phase diagram. Since the knowledge of phase equilibria is essential in designing new materials, determination of Gibbs free energy for respective phases is being continued on both theoretical as well as experimental ways. While in principle chemical potentials of pure substances are needed to derive Gibbs free energy of formation of the stoichiometric phases, it is not the case for the phase (solid or liquid) with variable composition. As an example, in Fig 1, ΔG_m for three different systems is shown. Fig.1a shows free energy of formation of the intermetallic, stoichiometric Mg_2Si phase recalculated per one mole of atoms (Turkdogan, 1980). Fig1b illustrates Gibbs energy of formation of one mole of liquid In-Pb solution (Hultgren, 1973). Finally, Fig.1c demonstrates Gibbs energy of formation of the solid phase, wustite ('FeO') (Spencer & Kubaschewski, 1978).

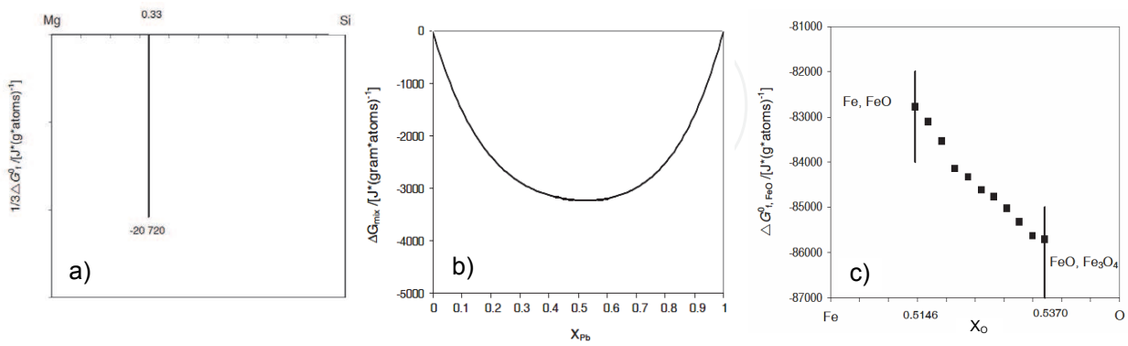

Fig. 1. Gibbs free energy of formation of a) stoichiometric Mg_2O phase, b) liquid In-Pb solution, c) solid phase 'FeO' wustite.

In the last two cases experimental information about chemical potentials of both components in the solution (partial Gibbs energies) was necessary to obtain ΔG_m vs. composition dependencies at fixed temperature.

In general, there are four experimental methods, namely calorimetry, vapour pressure, electrochemical and phase equilibration, one can use to obtain thermodynamic functions, which describe properties of respective phases, solid or liquid. Calorimetry is an indispensable tool to measure enthalpy changes , but its weakness consists in the fact that a number of calorimetric measurements must be combined in order to obtain Gibbs energy changes. Vapour pressure methods (both static and dynamic) cover wide range of vapour pressures from which standard free energy change as well as activities (chemical potentials) of components in the solution can be obtained. The most powerful modification of this technique is effusion method combined with mass spectrometry, which identifies and gives the partial pressure of all species present in the gas phase. Another advantage is the temperature of experiments, which cannot be matched by any other method. Partial Gibbs energy can also be derived from the investigation of equilibrium between different phases. In most cases the success of this method relies heavily on the accuracy of chemical analysis of phases involved in chemical equilibrium. Finally, an electrochemical method (so-called e.m.f. method) which is based on properly designed electrochemical cell can supply information about chemical potential of the components in any phase: gaseous, liquid or solid. Though, undoubtedly calorimetry is the most precise and direct method to measure heat effects of chemical changes i.e. enthalpy changes, chemical potential is needed to derive Gibbs free energy change. Both, e.m.f. and vapour pressure methods can yield chemical potential of the component through its activity measurements, but this approach has one weakness. Usually, we can measure activity for only one component in the solution. In good, old days Gibbs-Duhem equation was used to solve this problem and to derive activities for other components. In the age of modeling and computers this problem is solved much faster and the desired expression:

$$G_m = X_A \mu_A + X_B \mu_B + \ldots \quad (1)$$

(where X_i denotes mole fraction and μ_i denotes chemical potential)
for Gibbs free energy of one mole of the either solid or liquid phase can be easily obtained.
As far as the determination of the partial Gibbs energy of the components is concerned, in our opinion the electrochemical method may be considered as the most accurate one, though not without many traps. Ben Alcock used to say that e.m.f. method is the best method to derive activity of the component in the solution if…….works. This humorous and even a little spiteful comment is perhaps a good reason to discuss the principles and the range of applicability of this method.

2. Principles

When an electronic conductor (metal, semiconductor, polymer) is brought into equilibrium with ionic conductor (liquid electrolyte solution, molten salt, solid electrolyte, etc.) an interface between these two phases is created. Then, due to the charge separation between these two phases, the interface is charged and an electric potential difference Φ across the interface builds up. Such a two-phase system one may call the electrode (half-cell) and it can be schematically shown in Fig.2.
The change between the properties of the electronic and ionic conductors must take place over the certain distance (however small). Thus, instead of razor-sharp interface, it is better to think about an interphase region, which is a region of changing properties between

phases. In fact, this region decides about the charge transfer process between the two phases. This charge transfer process is the electrode reaction, and generally it takes place between oxidized and reduced species:

$$Ox + ze = Red \tag{2}$$

which in case of a metal M in contact with the solution containing its ions M^+ can be written as:

$$M^+ + e = M \tag{3}$$

From this electrode reaction results the potential buildup $\Phi_{M+/M}$ at the interface. It is assumed that this reaction is reversible (transfer of charge takes place with the same rate in both directions) and the Laws of thermodynamics can be applied to it. Leaving classification of various electrodes to electrochemists, let's see how this potential can be determined.

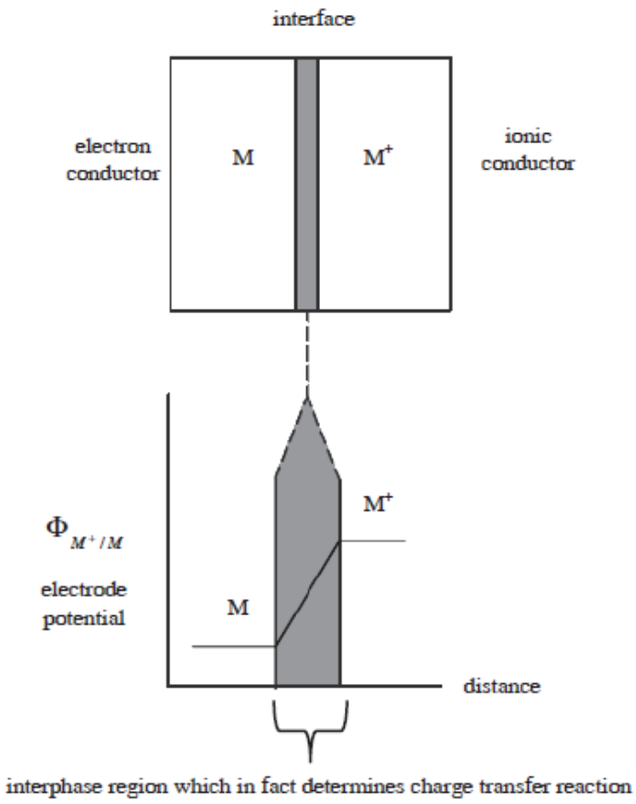

Fig. 2. Scheme of the electrode – electrolyte interface.

The answer to this problem is simple: we need another electrode which must serve as a reference. The single potential cannot be measured, but we can always measure its difference between two half-cells. Thus, the proper construction based on two electrodes yields the source of electric potential difference called electromotive force E (e.m.f.). Such a construction, which is schematically shown in Fig. 3, is called an electrochemical cell.

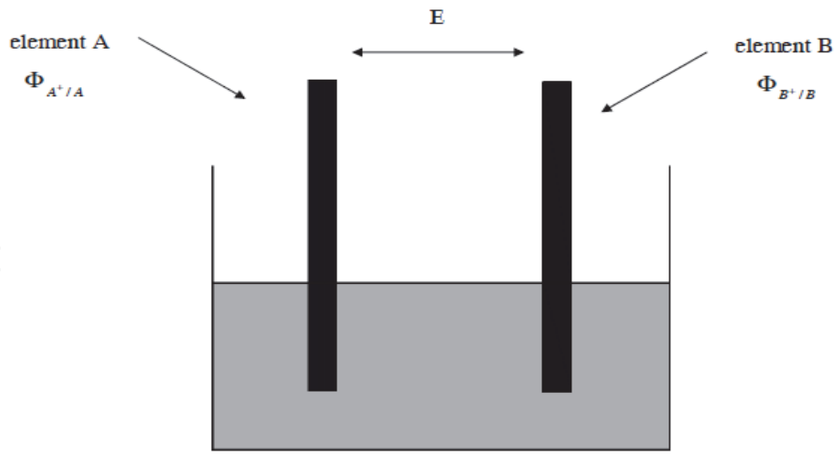

Fig. 3. General scheme of an electrochemical cell.

If this cell is not connected to the external circuit, its internal chemical processes are at equilibrium and do not cause any net flow of charge. Electrochemical energy can be stored. However, if it is connected, then under potential difference the charge must pass from the region of the lower to higher potential. Consequently, to force the charge to flow, work must be done. For any chemical process occurring under constant p and T, the maximum work that can be done by the system is equal to the decrease in its Gibbs free energy:

$$\text{work } W = -\Delta G \tag{4}$$

If this work is electrical one, it equals to the product of charge passed Q = zF and voltage E. For balanced cell reaction, which brought about the transfer of z moles of electrons, this work is given by:

$$W = zFE = -\Delta G \tag{5}$$

where E is cell's electromotive force. From this relationship, the change in Gibbs free energy for the reversible well defined chemical reaction which takes place inside the cell, can be determined as:

$$\Delta G = -zFE \tag{6}$$

where z is number of moles of electrons involved in the process and F is Faraday constant (i.e. the charge of one mole of electrons). Using well-known relations between ΔG, ΔH and ΔS one can express corresponding enthalpy and entropy changes through E vs. T dependence as:

$$\Delta S = zF(\partial E/\partial T)_p \tag{7}$$

and

$$\Delta H = -zFE + zFT\left(\partial E/\partial T\right)_p \tag{8}$$

Thus, from measured E vs.T dependence, all thermodynamic functions of the well-defined chemical process taking place inside the cell can be derived.

Under the assumption of chemical equilibrium , eq.6 can be also applied to the electrode reaction. Using the relationship between ΔG and an equilibrium constant K, which is:

$$\Delta G = \Delta G^0 + RT \ln K \tag{9}$$

and combining equations (6) and (9), one can arrive at Nernst's equation:

$$\Phi_{Ox/Red} = \Phi^0_{Ox/Red} - (RT/zF) \ln K \tag{10}$$

in which K is an equilibrium constant written for any electrode reaction in the state of equilibrium (in fact dynamic one). In eq.10, $\Phi_{Ox/Red}$ is an electrode potential, $\Phi^0_{Ox/Red}$ is standard electrode potential (all species taking part in the reaction are at unit activity) and z in a number of moles of electrons taking part in a charge transfer.
Having established all necessary dependencies for electrode potential one can ask how two half-cells can be combined to construct electrochemical cell, and how electromotive force E can be obtained in each case. The general scheme of the cell's classification is shown in Fig.4

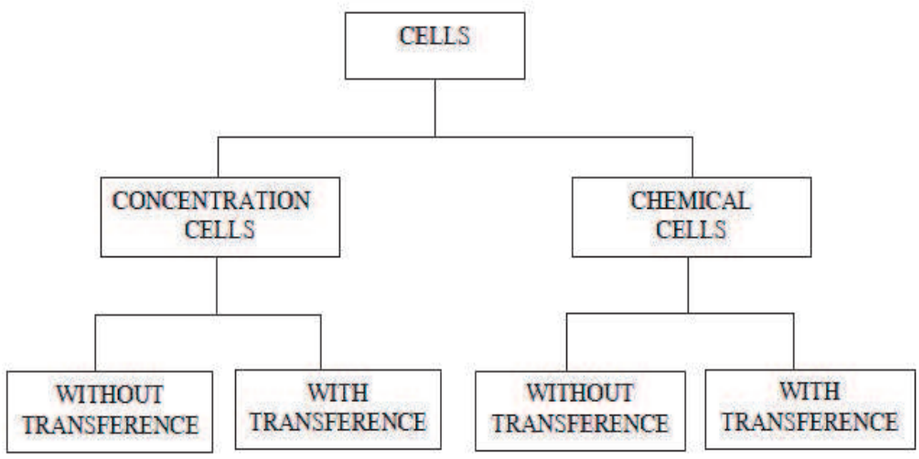

Fig. 4. Classification of the electrochemical cells.

This scheme is based on two characteristic features:

- the nature of the chemical process responsible for the electromotive force production,
- the manner in which the cell is assembled (i.e. where two half-cells are combined into one whole with or without the junction).

Following several simple rules, which say that:

- positive electrode is placed always on the right-hand side of each cell's scheme,
- electrode reactions are always written as reduction reactions,
- electromotive force E for each type of the cell is calculated as the difference of the electrode potentials:

$$E = \Phi_{right} - \Phi_{left} \tag{11}$$

one can analyze each type of the cell construction to see how E is developed, and what kind of thermodynamic information can it deliver.

3. Cells construction

3.1 Chemical cell without transference

We start our considerations from the chemical cells. Schematic representation of this kind of a cell is shown in Fig.5.

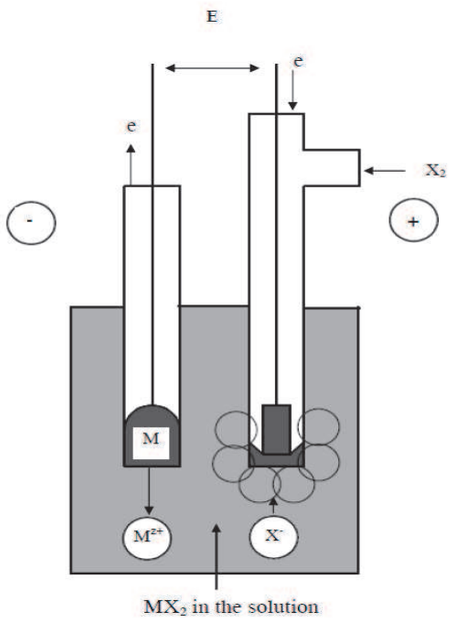

Fig. 5. Scheme of a chemical cell without transference.

Left-hand side electrode consists of the pure metal or alloy, which is immersed into the solution containing its cations (e.g. molten salt). Potential of this electrode written for the reduction reaction :

$$M^{z+} + ze = M \tag{12}$$

is

$$\Phi_{M^{z+}/M} = \Phi^{0}_{M^{z+}/M} - (RT/zF)\ln(a_M / a_{M^{z+}}) \tag{13}$$

On the right-hand electrode gas X_2 remines in contact with the liquid ionic phase fixing chemical equilibrium of the reaction:

$$(z/2)X_2 + ze = zX^- \tag{14}$$

and establishing the potential :

$$\Phi_{X^-/X_2} = \Phi^{0}_{X^-/X_2} - (RT/zF)\ln(a^{z}_{X^-} / p^{z/2}_{X_2}) \tag{15}$$

Consequently, according to the rule mentioned above, the electromotive force of the cell is:

$$E = \Phi_{X^-} - \Phi_{M^{z+}} = E^0 + (RT/zF)\ln(a_M p_{X_2}^{z/2} / a_{M^{z+}} + a_{X^-}^{z}) \quad (16)$$

Fixing X_2 pressure at the electrode (e.g. p_{X_2} = 1bar), and assuming that $a_{MX_z} = a_{M^{z+}} + a_{X^-}^{z}$, we have :

$$E = E^0 + (RT/zF)\ln(a_M / a_{MX_z}) \quad (17)$$

It is clear that this type of the cell can be used to measure activities of the components either in metallic or in ionic solution. It is also clear that overall cell reaction is:

$$\underline{M} + (z/2)\, X_2 = \underline{MX_z} \quad (18)$$

and a decrease of Gibbs free energy of this reaction is responsible for the e.m.f. production. The characteristic feature of this cell construction is **the same** liquid electrolyte solution in contact with both electrodes.

3.2 Chemical cell with transference

Another type of chemical cell is so-called Daniell-type cell, in which two dissimilar metals are immersed into two different liquid electrolytes forming two half-cells. To prevent these electrolytes from mixing and consequently, irreversible exchange reaction in the solution, they are separated by the barrier, which however must assure electric contact between both half-cells. The scheme of this cell is shown in Fig.6

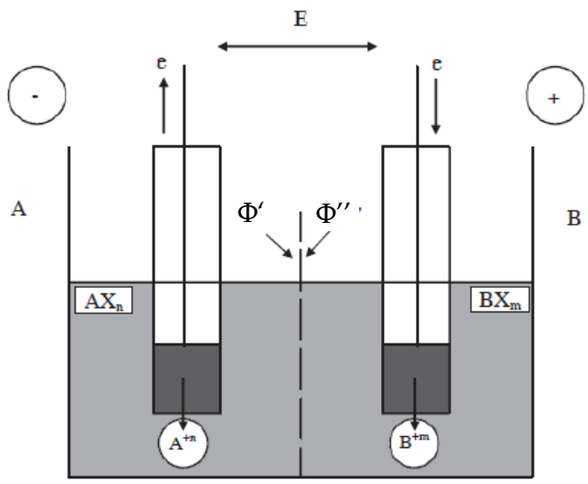

Fig. 6. Scheme of a chemical cell with transference.

The barrier called a junction can be liquid or solid (salt bridge, permeable diaphragm, ion-selective membrane) and can connect the half-cells in a number of different ways . Writing the reduction reaction at the electrodes as:

$$A^{n+} + ne = A \quad (19)$$

$$B^{m+} + me = B \tag{20}$$

and assuming that metals used in electrodes are pure, one can write the expression for electrode potentials:

$$\Phi_{A^{n+}/A} = \Phi^0_{A^{n+}/A} - (RT/nF)\ln(1/a_{A^{n+}}) \tag{21}$$

$$\Phi_{B^{m+}/B} = \Phi^0_{B^{m+}/B} - (RT/mF)\ln(1/a_{B^{m+}}) \tag{22}$$

The e.m.f. of this cell produced by the exchange reaction:

$$mA + nB^{m+} = nB + mA^{n+} \tag{23}$$

is

$$E = E^0 - (RT/zF)\ln(a^m_{A^{n+}}/a^n_{B^{m+}}) \tag{24}$$

where z = nm, activity of metals is equal to one, and expression under logarithm represents equilibrium constant K of the reaction (23). Thus, this cell may provide information about Gibbs free energy change of the exchange reaction at constant temperature, entropy and enthalpy changes can be also obtained if temperature dependence of the e.m.f. is measured. It is not very convenient for high temperature measurements, but can be used successfully while working with aqueous solutions, especially when one half-cell is set as the reference electrode. The characteristic feature of this type of cell is the separation of **two different** electrolytes with the junction assuring electrical contact, but preventing solutions from mixing. Consequently, since two more interfaces in contact with the solution appeared in the cell, there is a hidden potential drop across the junction
$E_{junction} = \Phi'' - \Phi'$ in measured E which not always can be precisely determined. Thus, measurements based on cells with transference may not give as accurate data as chemical cells.

3.3 Concentration cells without transference

If in the same electrolyte solution pure metal and its alloy are submerged, galvanic cell is created. Its scheme is shown in Fig. 7
Two electrode reactions can be written as:

$$M^{z+} + ze = M \tag{25}$$

on the l.h.s , and

$$M^{z+} + ze = \underline{M} \tag{26}$$

on the right, which is more positive.
Corresponding electrode potentials are:

$$\Phi_{M^{z+}/M} = \Phi^0_{M^{z+}/M} - (RT/zF)\ln(1/a_{M^{z+}}) \tag{27}$$

and

$$\Phi_{M^{z+}/\underline{M}} = \Phi^{0}_{M^{z+}/M} - (RT/zF)\ln(a_M / a_{M^{z+}}) \quad (28)$$

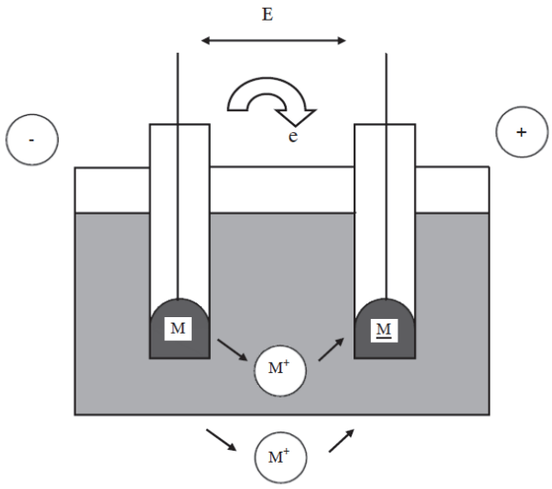

Fig. 7. Scheme of a concentration cell without transference.

The net cell reaction in this case is:

$$M = \underline{M} \quad (29)$$

and E of this cell is generated by the concentration (chemical potential) difference, and has the final form:

$$E = -(RT/zF)\ln a_M \quad (30)$$

since activity of metal cations is fixed and standard electrode potentials for both electrodes are the same ($E^0 = 0$). From equations (30) and (6) after rearrangement one may obtain:

$$RT \ln a_M = -zFE = \Delta G_m \quad (31)$$

Thus, the free energy change of the transfer process from pure state into the solution can be derived directly from measured E. It is probably the most convenient way to obtain partial function of the alloy component. If the E vs.T dependencies are linear (i.e. E = a+bT), partial entropy and partial enthalpy for the process (29) can be obtained directly for a given composition of the alloy from eqs. (7) and (8):

$$\Delta S_M = zFb \quad (32)$$

$$\Delta H_M = -zFa \quad (33)$$

Again, characteristic feature of this cell is **the same** electrolyte with fixed concentration of M^{z+} ions for both electrodes and the missing junction.

3.4 Concentration cells with transference

The last type of cell is based on the junction which is selectively conducting with one type of an ion. Two versions of this type of cell are schematically shown in Fig. 8. Let's consider the

construction given in Fig.8a. Two identical metals (in Fig.8b two identical gaseous species) which are shown are in contact with two electrolyte solutions of two different compositions. These two half-cells are connected through the cation (anion) conducting membrane.

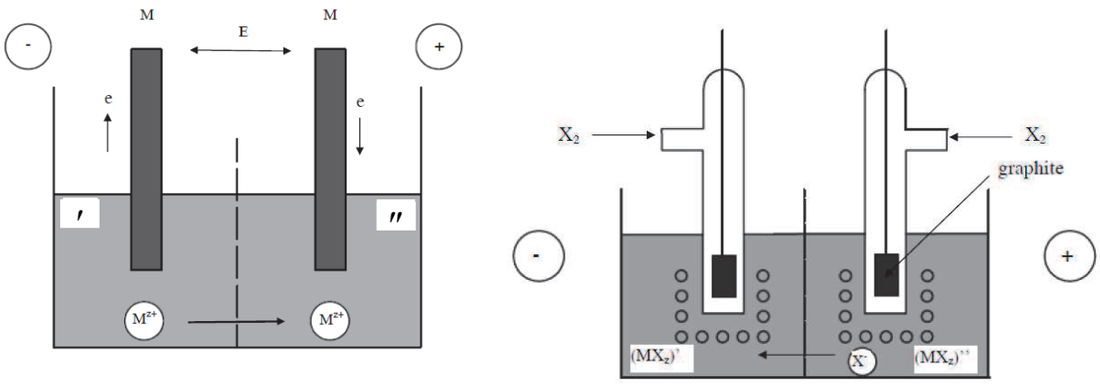

Fig. 8. Scheme of a concentration cell with transference: a) cation conductivity membrane, b) anion conductivity membrane.

If concentration of cations is such that on l.h.s it is higher (a' > a'') than on the right side, diffusion of cations will proceed and it sets up electric potential difference across the membrane. This potential gradient eventually will stop diffusion and equilibrium is reached. Due to cations migration to the right side, this electrode is more positive. Writing reduction reactions on both electrodes as:

$$(MX)' + e = M + X^- \tag{34}$$

and

$$(MX)'' + e = M + X^- \tag{35}$$

one can express electrode potentials as:

$$\Phi' = \Phi^{0'} - (RT/F)\ln(a_{X^-}/a_{MX'}) \tag{36}$$

$$\Phi'' = \Phi^{0''} - (RT/F)\ln(a_{X^-}/a_{MX''}) \tag{37}$$

Again, since both standard potentials are identical and activity of X^- will not change due to the action of ion- selective membrane which stops their transfer, e.m.f. of this cell (similar reasoning can be given for the cell shown in Fig.8b) is:

$$E = (RT/F)\ln(a_{MX''}/a_{MX'}) \tag{38}$$

If on left side of the cell there is pure MX, then e.m.f. gives directly activity of MX in the solution. However, one must remember that measured E has again an internal contribution from the voltage drop across the junction. Having described principles of cells operation and construction, let's have a brief look at the beginning of the story.

3.4.1 The road to solid electrolytes

Probably, the first-ever type of cells employed to e.m.f. measurements in molten salts was Daniell – type cell employed by Sackur (1918). Relatively easy to construct while working with aqueous solutions, it faced difficulty when temperature of the cell operation was raised. At high temperatures it was used to study molten salts. Concentration cells without transference appeared to be more convenient to study metallic systems. Consequently, this kind of research was initiated by Taylor (1923) and Seltz (1935). Working with cells with transference the main problem connected with this construction was a junction between half-cells and generated junction potential. To avoid interactions between different solutions a number of coupling was tried to assure the electrical contact between the half-cells. While in aqueous solutions the salt bridge was (and still is) the best solution, at high temperature this particular connection brought about same problems. Examples of different half-cell connections tried in the past are shown in Fig.9.

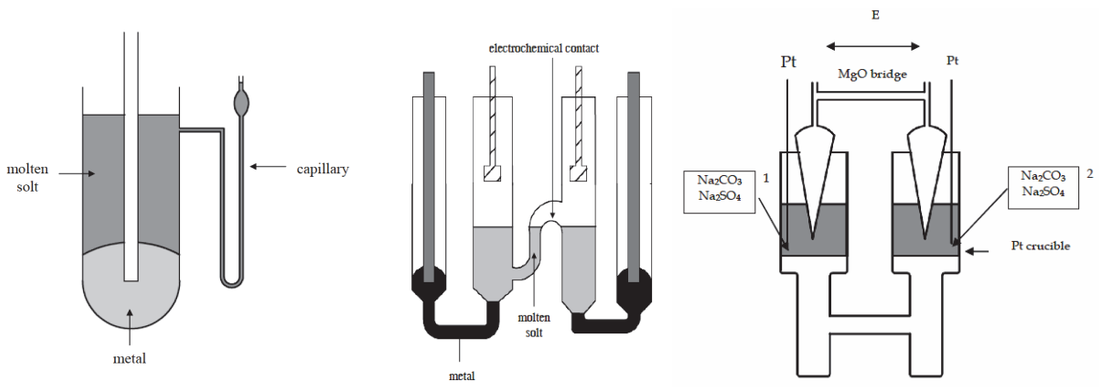

(a) (b) (c)

Fig. 9. Different construction of a bridge joining half cells: a) capillary bridge after Lorenz & Michael (1928), b) density difference after Holub et al (1935), c) MgO soaked in molten salt after Flood et al (1952).

In this Figure junctions employed by Lorenz & Michael (1928), Holub et al in 1935 and Flood et al in 1952 are shown. The main problem was to estimate $E_{junction}$ in each case.
In approximately the same time Salstrom (1933) and next Salstrom and Hildebrandt (1930) initiated a series of investigations of molten salts using chemical cells. It was soon realized that proper combination of two chemical cells e.g. $M_1/M_1X/X_2$ and $M_2/M_2X/X_2$ should in principle yield the result equivalent to the result of an exchange reaction completed in the concentration cell $M_1/M_1X//M_2/M_2X$. These findings stimulated both: development of chemical cells which became a source of thermodynamic data for pure substances as well as their solutions, and also employment of concentration cells to provide not only the data for systems for which chemical cells could not be assembled, but also to study the junction potential itself. Its value apparently varied depending on a junction's construction. It appeared to be small for the liquid junction, but as shown by Tamman (1924) who used the cell Ag,AgCl/ glass /$PbCl_2$,Pb, it could be quite significant. Thus, the nature of the junction : liquid or solid, mechanical (frit, gel) or ion-conducting (glass) apparently played significant role in the generated potential drop across the junction. Though experiments with solid substances which played part of electrolytes were already under way, the theory was needed to explain observed discrepancies.

Carl Wagner (1933, 1936) derived the expression for the steady - state ,open – circuit voltage across the scale of solid inorganic compound. Being Walter Schottky's student ,Wagner with his characteristic brightness realized the importance of the defect structure of the solids and its influence on the conductivity. He put forward the theory which gave foundations of the knowledge necessary to design materials, today called solid electrolytes. However, he had to wait almost 25 years to demonstrate applicability of this concept in thermodynamic measurements. In the pioneering work with Kiukkola (1957) they demonstrated that zirconium oxide doped with CaO can be used as the solid electrolyte conducting with oxygen ions. His theory in the simplified version can be explained today in the framework of non-equilibrium thermodynamics.
Let's suppose that through the layer of an inorganic material three species: cations C, anions X and electrons e can migrate. According to Onsager's theory in 1931 their fluxes can be described by the equations:

$$J_C = L_{CC} \text{ grad } \mu_C + L_{CX} \text{ grad } \mu_X + L_{Ce} \text{ grad } \Phi \quad (39)$$

$$J_X = L_{XC} \text{ grad } \mu_C + L_{XX} \text{ grad } \mu_X + L_{Xe} \text{ grad } \Phi \quad (40)$$

$$I_e = L_{eC} \text{ grad } \mu_C + L_{eX} \text{ grad } \mu_X + L_{ee} \text{ grad } \Phi \quad (41)$$

where gradients of chemical potential and electric field play the role of forces responsible for the flow of species and charge through the layer. In the linear regime the matrix of linear coefficients is symmetric i.e. $L_{ij} = L_{ji}$. For the open circuit electric current is zero i.e. $I_e = 0$, and from eq.41 one can obtain:

$$- \text{grad } \Phi = (L_{eC}/L_{ee}) \text{ grad } \mu_C + (L_{eX}/L_{ee}) \text{ grad } \mu_X \quad (42)$$

In turn, if there is no gradient of chemical potentials in the system, and the charge flow is caused by the gradient of electric field, taking the ratio of total current and ion fluxes one can arrive at the expressions:

$$J_C / I_e = (L_{Ce} / L_{ee}) \quad \text{and} \quad J_X / I_e = (L_{Xe} / L_{ee}) \quad (43)$$

Introducing transference numbers defined as $I_C/ I_e = t_C = z_C F J_C / I_e$ and $I_X / I_e = t_X = z_X F J_X/ I_e$, and taking into account reciprocal relations $L_{ij} = L_{ji}$, one can rewrite the equation (42) in the following form:

$$- \text{grad } \Phi = (t_C / z_C F) \text{ grad } \mu_C + (t_X / z_X F) \text{ grad } \mu_X \quad (44)$$

If inorganic material is conducting only with anions, transference numbers do not depend on chemical potential, and $t_X = 1 – t_e$, then eq.44 can be integrated across the inorganic layer to yield:

$$\Phi'' - \Phi' = E = - \{(1- t_e)/ z_X F\} d\mu_X \quad (45)$$

In the absence of electronic conductivity in the material ($t_e = 0$), and for gaseous species X_2 for which $\mu_X = \mu_X^0 + RT\ln p_{X_2}$, one can arrive at the general formula:

$$E = (RT/z_X F)\ln\left\{ p''_{X_2} / p'_{X_2} \right\} \quad (46)$$

Using equation (44) it is also easy to show how liquid junction potential ($E_{junction}$) is generated. Let's assume that instead of the inorganic solid layer, there is the liquid interphase layer between two solutions. In this liquid phase dissociating electrolyte CX yields ions C^{z+} and X^{z-}, which may move independently through the liquid. Then, from (44) one obtains:

$$E_{junction} = - RT/F \ (t^{+}/z^{+}) \ d\ln a_{+} - RT/F \ (t^{-}/z^{-}) \ d\ln a_{-} \quad (47)$$

Having $z^{+} = 1$ and $z^{-} = -1$, and assuming for the aqueous solution $a_{+} = a_{-} = c_{CX}$, equation (47) can be rearranged and integrated along the layer to yield:

$$E_{junction} = -(RT/F) \ (t^{+} - t^{-}) \ \ln \{ c_2 / c_1\} \quad (48)$$

It is clear that for equal transference numbers (i.e. mobility) the potential drop across the junction is nil.

Since the time of Wagner's paper a number of excellent elaborations was devoted to the solid electrolytes field (Alcock, 1968; Rapp & Shores, 1970; Goto & Pluschkell, 1972; Subbarao, 1980), and we are not going to compete with them. Instead, we'd like to present those areas of research in which, using solid electrolytes, we were able to obtain new data and to small extend we contributed to the extension of the knowledge about thermodynamic properties of high temperature systems.

3.4.2 Oxygen in dilute liquid solutions

To describe the solute element behavior over dilute solution range, free energy interaction coefficients were introduced. However, experimental evidence gathered so far is mainly limited to copper and iron alloys. Working on the review which summarized up to 1988 the data on the solubility of oxygen in liquid metals and alloys (Chang et al, 1988) we found out that there is virtually no information about solute-oxygen interaction in the liquids from which $A_{III}B_{V}$ semiconducting crystals are grown. The problem is not trival since electrical and optical properties of so–called III-V compounds are influenced by oxygen or water vapor in the growth environment. Oxygen incorporated into crystal brings about a decrease in carrier concentration, photoluminescence efficiency and deterioration of surface morphology. Thus, severe requirements regarding purity of crystals grown from the liquid phase stimulate the need for the data on thermodynamics of solutions containing oxygen dissolved in III-V alloys.

The application of the coulometric titration method to the study of oxygen solubility in liquid metals was first initiated by Alcock and Belford in 1964, and further developed by Ramanarayanan and Rapp in 1972. Our experimental method and the procedure can be described briefly in the following way. Using the electrochemical cell of the type:

$$W, A - B - O \ / \ O^{2-} \ / \ air, Pt \quad I$$

titrations were carried out in the chosen temperature range, which depended on the system studied. In this cell A denotes In and Ga, while B denotes As and P. AB alloys of the chosen composition were prepared in evacuated and sealed silica capsules by melting oxygen free metals with respective MX compounds. Samples were kept at constant temperature for 24 h and then quenched. The tube of the solid electrolyte contained between 2 and 3 g of metallic alloy. A tungsten wire acted as an electric contact with a metal electrode. The outer part of the solid electrolyte tube coated with platinum paste worked as an air reference electrode

and was connected to the electric circuit with a platinum wire. The electric circuit contained a potentiostat with a charge meter and digital voltmeter. Purified argon was allowed through the cell just above the surface of the liquid metal. The schematic cell I arrangement is shown in Fig. 10.

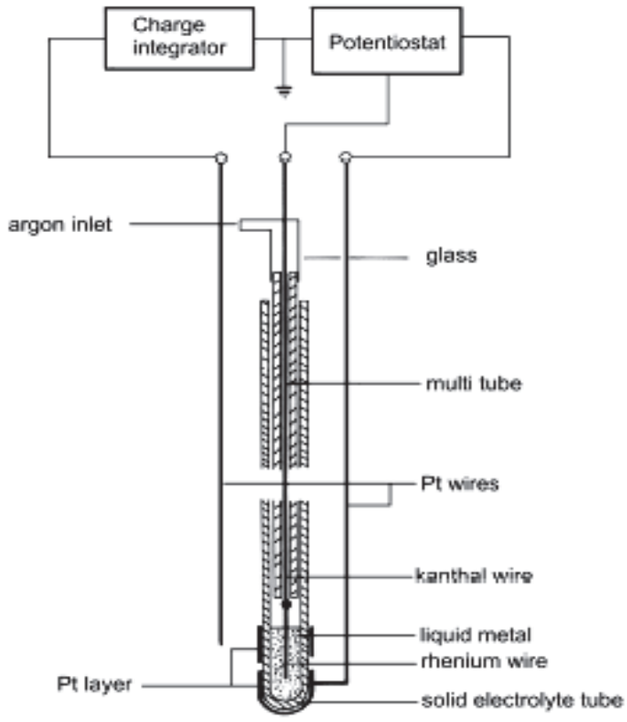

Fig. 10. Scheme of electrochemical cell with air reference electrode by Wypartowicz & Fitzner (1987).

After the equilibrium electromotive force of the cell E_1 had been recorded, the preselected additional potential ΔE was applied by the potentiostat. The resulting current passed through the cell in such a direction that oxygen was pumped out of the alloy. The decrease in oxygen concentration resulted in an increase of the e.m.f. of the cell and a decay of the electric current. The final e.m.f. value E_2 and the electric charge passed Q were recorded. The experimental run was repeated several times at the same temperature, then the temperature was changed.
Activity coefficients of oxygen in liquid alloys were calculated from:

$$f_0 = p_{O_2}^{1/2} / C_{O(1)} \tag{49}$$

where p_{O2} is directly related to the initial e.m.f. through the equation:

$$E_1 = (RT/2F)\ln(0.21/p_{O_2})^{1/2} \tag{50}$$

and the oxygen concentration $C_{O(1)}$ can be obtained from two equations:

$$C_{O(1)} - C_{O(2)} = 100\ (M/W)(Q_{ion}/2F) \quad (51)$$

and

$$E_2 - E_1 = (RT/2F)\ \ln\ (C_{O(1)}/C_{O(2)}) \quad (52)$$

where $E_2 - E_1 = \Delta E$ is an imposed potential difference and the oxygen concentration is expressed in atomic per cent. To obtain eq. 52, Henry's Law was assumed to obey.
In above equations Q_{ion} is the charge corrected by the amount caused by electronic conductivity, M is mass of the sample, and W is atomic weight of the alloy. Experiments were run under following conditions:

- oxygen concentration was kept in the range from 10^{-2} to 10^{-3} atomic percent in order to minimize possible evaporation of oxide species,
- solute concentration varied from 0.01 up to 0.07 X_{As} and 0.05 X_P,
- temperature of experiments (depending on the system) was chosen between 1023 and 1373 K,
- only pump-out experiments were performed.

SYSTEM	ε_0^i	Temperature range	Reference
In-As-O	$31.47 - (39635\ /\ T)$	1023-1123 K	Wypartowicz & Fitzner, 1987
In-P-O	$.\ 589.4 - (803435\ /\ T)\ .$	1100-1200 K	Wypartowicz & Fitzner, 1990
Ga-As-O	$21.10 - (37046\ /\ T)$	1123-1223 K	Wypartowicz & Fitzner, 1988
Ga-P-O	$59.00 - (39635\ /\ T)$	1323-1373 K	Onderka et al, 1991

Table 1. Interaction parameters determined in dilute A-B-O solutions.

Experimental results obtained for four diluted systems, namely In-As-O (Wypartowicz & Fitzner, 1987), Ga-As-O (Wypartowicz & Fitzner, 1988), In-P-O (Wypartowicz & Fitzner, 1990) and Ga-P-O (Onderka et al, 1991) are shown in Table 1. In all cases solute addition decreases activity coefficient of oxygen. This decrease however is the result of a subtle interplay of interactions between A-B atoms on one hand, and A-O and B-O atoms on the other.

3.4.3 Stability of high-temperature ceramic superconductors

The discovery of high temperature ceramic superconductor by Bednorz and Muller (1986) stimulated worldwide research of this type of oxide systems. Research efforts concentrated soon on Y-Ba-Cu-O system, in which $YBa_2Cu_3O_{7-x}$ phase with perovskite structure (designated as Y<123>) showed transition temperature above 90 K (Wu et al, 1987). It was very quickly demonstrated that substitution of yttrium by other rare earth elements is possible. Since the knowledge of phase equilibria in the copper oxide-barium oxide-lanthanide sesquioxide system is necessary for successful synthesis of respective phases, phase stability as a function of temperature and oxygen partial pressure is required to define processing conditions. It appeared however, while working on the Y-Ba-Cu-O system

(Fitzner et al, 1993), that Gibbs free energy of formation of *Ln*<123> phase (*Ln* is a symbol of any lanthanide element) cannot be obtained directly from the e.m.f's produced by the cell with zirconia electrolyte. More sophisticated strategy must be adopted to achieve this aim, and another cell with CaF_2 solid electrolyte must be employed. The measurements require three steps which are schematically shown in Fig. 11.

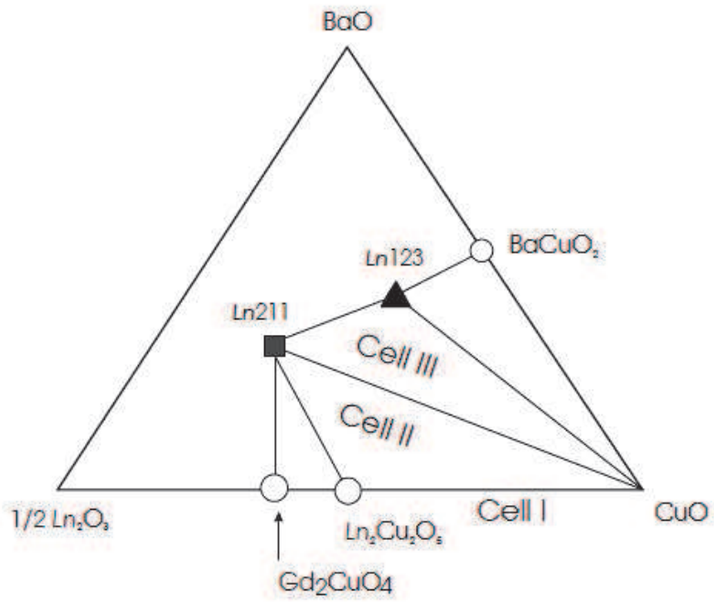

Fig. 11. Scheme of phase equilibria leading of subsequent cells construction.

Cell I is assembled to measure the stability of phases existing in CuO-Ln_2O_3 systems. It is based on zirconia electrolyte and essentially in its construction does not differ much from the cell employed to study liquid dilute solutions (Fig.10). The only substantial difference consists in the working electrode, which in this case is a mixture of oxides. Depending on the size of the lanthanide atom there are two phases which can exist at high oxygen pressure: $CuLn_2O_4$ and $Cu_2Ln_2O_5$. Under decreasing oxygen pressure some of them can be reduced to delafossite – type $CuLnO_2$ .In a series of experiments we determined Gibbs free energy of formation of a number of phases resulting from the reaction between CuO and respective lanthanide oxides. The results of these investigations are summarized in Table 2.
Having established $\Delta G^0_{\text{oxides}}$ in CuO – Ln_2O_3 systems we could proceed with cell II. It operates with the working electrode CuO–(CuO + Ln_2O_3) phase –Ln_2BaCuO_5 phase (designated as *Ln*<211>). To put this cell into operation, CaF_2 solid electrolyte is required.
The application of CaF_2 – type electrolyte in e.m.f. cells employed to the study of oxide systems was described in details by Levitskii in 1978. The cell construction used in our study followed that used by Alcock and Li in 1990. The cell assembly and the whole experimental setup are schematically shown in Fig. 12

Ln	$\Delta G^0_{f,\,oxide} = A + B*T$ [J*mol^{-1}]			Reference
	$Cu_2Ln_2O_5$	$CuLn_2O_4$	$CuLnO_2$	
Lu	39390 – 38.17*T			Przybyło & Fitzner, 1996
Yb	19429 – 22.02*T			Kopyto & Fitzner, 1996
Tm	35275 – 34.09*T			
Er	17427 – 19.61*T			
Ho	18165 – 19.49*T			
Dy	16648 – 17.58*T			
Gd		9562 – 12.29*T		Fitzner, 1990
Eu		885 – 8.67*T	-6640 + 4.02*T	Onderka et al. 1999
Sm		-23500 + 11.06*T	-11250 + 9.64*T	Kopyto et al. 2003
Nd		-28620 + 10.85*T	-18990 + 15.21*T	
Y	6670 – 7.05*T		-7265 + 8.31*T	Przybyło & Fitzner, 1995

Table 2. Thermodynamic data obtained for phase existing in Cu-*Ln*-O systems.

The main part of the cell consists of the spring system which was responsible for pressing together working electrode, CaF_2 single crystal and the reference electrode inside the silica tube filled with flowing, synthetic air. The cell was placed in a horizontal resistance furnace which temperature was controlled by an temperature controller. Dry, synthetic air was used to assure that no the traces of moisture can get into the cell compartment. The equilibrium e.m.f. values, which were recorded by an electrometer, were attained in 3 to 10 hours depending on temperature. The platinum lead wires did not show signs of reaction with the electrode pellets after the experiments. Conventional ceramic methods were used to prepare respective phases. Weighed amounts of powders of $BaCO_3$, and CuO were mixed with respective lanthanide oxides, palletized and sintered in the stream of dry oxygen usually at about 1223 K. The e.m.f. measurements were carried out in several cycles of increasing and decreasing temperature. Thermal cycling of the cell produced virtually the same e.m.f. values after reaching constant temperature. The reversibility of the cell performance was also checked by passing the current of 0.1 mA from an external source for about 30 s. The e.m.f. returned to the original values within +/- 1 mV in about 1 – 5 minutes depending on temperature. The whole experimental cycle of the cell operation usually took about one week.
The following electrochemical cells were assembled:

$$CuO + Cu_2Ln_2O_5 + Ln\langle 211\rangle + BaF_2 \,/\, CaF_2 \,/\, CaO + CaF_2 \qquad \text{II}$$

for *Ln* = Yb, Tm, Er, Ho, Dy , and

$$CuLn_2O_4 + Ln\langle 211\rangle + Ln_2O_3 + BaF_2 \,/\, CaF_2 \,/\, CaO + CaF_2 \qquad \text{III}$$

for *Ln* = Gd, Eu, Sm and Nd. Either air or oxygen-argon mixture were flowed continuously through the cell vessel.

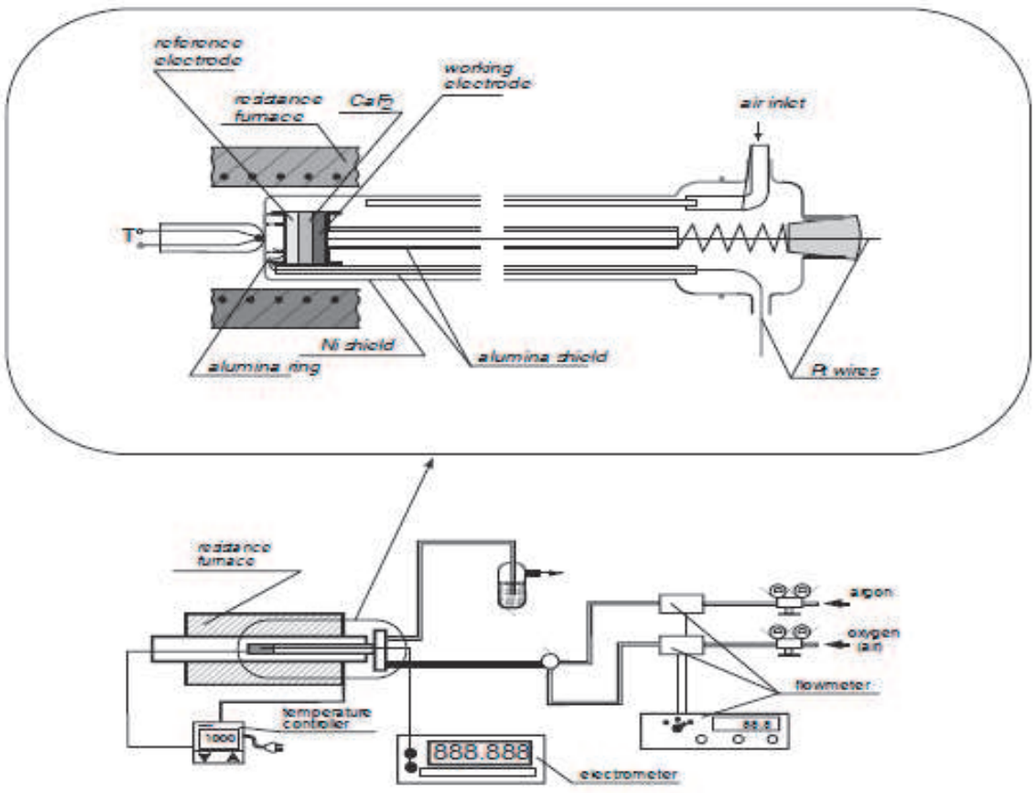

Fig. 12. Scheme diagram of the galvanic cell after Kopyto & Fitzner (1999).

The net reaction for the cell II is:

$$Ln\langle 211\rangle + CuO + CaF_2 = Cu_2Ln_2O_5 + BaF_2 + CaO \quad (53)$$

while for cell III :

$$Ln\langle 211\rangle + CaF_2 = CuLn_2O_4 + BaF_2 + CaO \quad (54)$$

Since mutual solubility between solid phases in the investigated temperature range is small, all components of reactions are essentially in the pure state. Thus, Gibbs free energy change of net cell reactions can be calculated as :

$$\Delta G^0 = -2F\,E \quad (55)$$

If obtained ΔG^0 equations are combined with Gibbs free energy change of exchange reaction between CaO and BaF_2, and also with respective changes of ΔG^0 for reactions of formation of respective double oxides, one can derive Gibbs free energy change for the reaction:

$$CuO + BaO + Ln_2O_3 = Ln\langle 211\rangle \quad (56)$$

Obtained $\Delta G^0_{oxides} = f(T)$ equations are gathered in Table 3
It is the last information needed to set the cell III. It operates with the working electrode: CuO–*Ln*<211> - *Ln*<123>.

Ln	$\Delta G^0_{f,Ln_{<211>}} = A + B * T$ [J*mol^{-1}]	Reference
Yb	-54900 – 4.85*T	Kopyto & Fitzner, 1997
Tm	-51500 – 5.00*T	
Er	-59300 – 1.66*T	
Ho	-52700 – 7.65*T	
Dy	-51200 – 9.06*T	
Gd	-59900 – 1.58*T	
Eu	-82530 + 16.50*T	Przybyło et al., 1996
Sm	-110580 + 41.29*T	Onderka et al, 1999
Nd	-137880 + 65.18*T	Kopyto et al, 2003

Table 3. Thermodynamic data obtained for respective *Ln*<211> phase.

The following electrochemical cells were assembled:

$$CuO + Ln<211> + Ln<123> + BaF_2 \,/\, CaF_2 \,/\, CaO + CaF_2 \quad (57)$$

for *Ln* = Yb, Tm, Er, Ho, Dy, Gd and Eu.
and their overall cell reaction is:

$$3CaF_2 + 2Ln<123> = 3CaO + 5CuO + 3BaF_2 + Ln<211> + (0.5 - x)\, O_2 \quad (58)$$

for which the change in Gibbs free energy can be written as:

$$\Delta G^0 = -\, 6F\, E - (0.5 - x)\, RT \ln p_{O2} \quad (59)$$

Combining reaction (58) with the exchange reaction between CaO and BaF_2, and with the reaction of formation of *Ln*<211> phases from oxides, one can arrive at the reaction of formation of *Ln*<123> phase from oxides and oxygen:

$$\tfrac{1}{2}\, Ln_2O_3 + 2BaO + 3CuO + (0.25 - x/2)\, O_2 = Ln<123> \quad (60)$$

Obtained $\Delta G^0 - (0.25 - x/2)\, RT \ln p_{O2} = f(T)$ equations for subsequent *Ln*<123> phases are gathered in Table 4.

Ln	$\Delta G^0 - (0.25 * \frac{1}{2} x) * RT * \ln(p_{O_2}) = A + B * T$ [J*mol^{-1}]	Reference
Yb	-133184 + 16.63*T	Kopyto & Fitzner 1999
Tm	-115143 + 3.96*T	
Er	-122728 + 7.01*T	
Ho	-118424 + 3.23*T	
Dy	-121883 + 7.13*T	
Eu	*-163250 + 44.70*T*	Przybyło et al., 1996

Table 4. Thermodynamic data obtained for respective *Ln*<123> phase.

Dependence of x = f(T) is required under fixed pressure to calculate the correction term. In case of Gd-phase the cell did not work reversibly, probably due to BaF_2*GdF_3 compound formation. In case of Eu, the result should be taken with caution. For elements with the radius smaller than Gd^{3+}, another phase designated as *Ln*<336> appears in the oxide system, and it is a matter of dispute weather this phase is separated from *Ln*<123> by two-phase region or it is simply a solid solution extending from *Ln*<123> phase.

4. Thermodynamic properties of liquid silver alloys

Taking part in two COST projects (531 and MP0602), which were devoted to the search of new lead-free solders, we were involved in the investigations of silver alloys. After all , Poland is a big silver producer and silver alloys seemed to be a reasonable choice. Consequently, using solid oxide galvanic cells with YSZ zirconia electrolyte (ZrO_2+Y_2O_3) the thermodynamic properties of a number of the liquid silver alloys were determined. Generally, this kind of galvanic cell can be described by the following schema:

electric contact, working electrode/YSZ electrolyte/reference electrode, electric contact

where the working electrode is metallic alloy of chosen composition mixed with the powder of metal oxide, and the reference electrode is powder mixture of the type Me+MeO or air. First of all in this kind of measurements, the $\triangle G^0_{f,MeO}$ of oxides for each component of the alloy must be known. Next, the activity of this metal which has the most stable oxide can be investigated. Second very important case in these measurements is a lack of an exchange reaction between components of the alloy and metal oxide which is used in this experiment. If Gibbs free energy of formation of two oxides is close to each other the exchange reaction may take place. In this case, the additional experiment must be done to clarify the possibility of an exchange reaction. If these conditions are fulfilled, the chosen silver alloys can be investigated by using e.m.f. method with YSZ zirconia electrolyte. From measured electromotive force E as a function of temperature for alloys of different compositions, the activity of the component of liquid silver alloy can be determined.
The following binary and ternary liquid silver alloys were investigated by using e.m.f. method with YSZ solid electrolyte: Ag-Bi (Gąsior et al., 2003), Ag-Sb (Krzyżak & Fitzner, 2004), Ag-In (Jendrzejczyk & Fitzner, 2005), Ag-Ga (Jendrzejczyk-Handzlik & Fitzner, 2011), Ag-Bi-Pb (Krzyżak et al., 2003), Ag-In- Sb (Jendrzejczyk-Handzlik et al., 2006), and Ag-In-Sn (Jendrzejczyk-Handzlik et al., 2008). In Table 5 galvanic cells which were used during measurements performed of various liquid silver alloys and the range of temperature in which measurements were done are given.

Alloy	Temperature of measurements	Galvanic cell
Ag-Bi	544-1443 K	W, Ag_x-$Bi_{(1-x)}$,Bi_2O_3/ZrO_2+Y_2O_3/NiO, Ni, Pt
Ag-Sb	950-1100 K	Re+kanthal, Ag_x-$Sb_{(1-x)}$, Sb_2O_3/ZrO_2+Y_2O_3/ air, Pt
Ag-In	950-1273 K	Re+kanthal, Ag_x-$In_{(1-x)}$, In_2O_3/ZrO_2+Y_2O_3/ NiO, Ni, Pt
Ag-Ga	1098-1273 K	Re+kanthal, Ag_x-$Ga_{(1-x)}$, Ga_2O_3/ZrO_2+Y_2O_3/ FeO, Fe, Pt
Ag-Bi-Pb	848-1123 K	Re+kanthal, Ag_x-Bi_y-$Pb_{(1-x-y)}$, PbO/ZrO_2+Y_2O_3/ air, Pt
Ag-In-Sb	973-1200 K	Re+kanthal, Ag_x-In_y-$Sb_{(1-x-y)}$, In_2O_3/ZrO_2+Y_2O_3/ NiO, Ni, Pt
Ag-In-Sn	973-1273 K	Re+kanthal, Ag_x-In_y-$Sn_{(1-x-y)}$, In_2O_3/ZrO_2+Y_2O_3/ NiO, Ni, Pt

Table 5. Galvanic cells which were used during measurements with silver alloys.

A schematic representation of the cell assembly which was used in measurements of liquid silver alloys is shown in following Fig. 13.

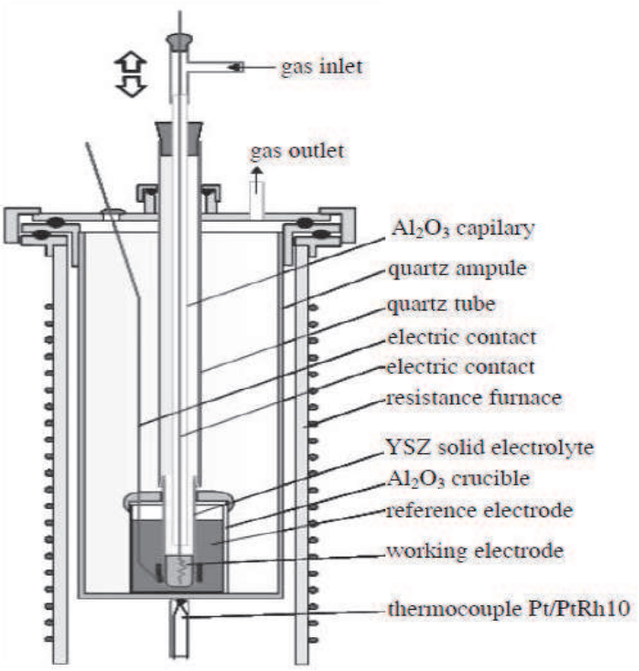

Fig. 13. Galvanic cell assembly after Jendrzejczyk & Fitzner (2005).

The tube of the solid zirconia electrolyte contained a liquid silver alloy of chosen composition. A small amount of pressed metal oxide was placed at the bottom of a YSZ tube. The metallic wires acted as an electric contact with the liquid metal electrode. A solid electrolyte tube was inserted into an alumina crucible filled with reference electrode which was a mixture of metal and oxide powders (in case of measurements with Ag-Sb and Ag-Bi-Pb the reference electrode was air. The construction of the cell was changed and this kind of the cell construction is shown in Fig.10). It was sealed inside the crucible with an alumina cement. Next, the whole cell was placed inside a silica tube, which was suspended on an upper brass head closing the silica tube. The cell was kept in a constant temperature zone of the resistance furnace. The measurement were carried out at increasing and decreasing temperature for several days. To check the reproducibility of the cell performance within the investigated temperature range, measurement were carried out on both heating and cooling cycles. For the reversible overall cell reaction the change Gibbs free energy $\triangle G$ was derived from the equation (6). Consequently, by combining equations which describe $\triangle G$ and $\triangle G^0_{f,MeO}$ we can obtain equation describing the activity of metallic component in liquid silver alloy. Next all thermodynamic properties of the liquid solution were described in the following manner.

The model for the substitutional solution was used to express the Gibbs free energy of mixing in the following form:

$$G^M = X_1G^0_1 + X_2G^0_2 + \ldots + RT(X_1\ln X_1 + X_2\ln X_2 + \ldots) + G^E \quad (61)$$

where parameters G^0_i denote the free energy of pure component "i" and are taken from the SGTE database (Dinsdale, 1991). The function G^E denotes the excess free energy and for binary system it is described by the Redlich-Kister formula (Redlich & Kister, 1948):

$$G^E_{1,2} = X_1(1\text{-}X_1)[L^0_{1,2} + (1\text{-}2X_1)^1L^1_{1,2} + (1\text{-}2X_1)^2L^2_{1,2} + \ldots] \quad (62)$$

For the ternary system, G^E (the excess free energy) is described by the Redlich-Kister-Muggianu polynomial (Muggian et al, 1975):

$$G^E_{1,2,3} = X_1X_2(L^0_{1,2} + L^1_{1,2}(X_1\text{-}X_2)) + X_1X_3(L^0_{1,3} + L^1_{1,3}(X_1\text{-}X_3)) + X_2X_3(L^0_{2,3} + L^1_{2,3}(X_2\text{-}X_3))$$
$$+ X_1X_2X_3(X_1\,L^0_{1,2,3} + X_2\,L^1_{1,2,3} + X_3\,L^2_{1,2,3}) \quad (63)$$

In above equations the x_i is the mole fraction of the components in an alloy and parameters $L^i_{1,2}$ and $L^i_{1,2,3}$ are linearly dependent on temperature and are given in J/mol*atom.
For subsequent silver alloy shown in Table 5 these parameters were calculated by using experimental data gathered for each system including those which were obtained from our e.m.f. measurements. Parameters $L^i_{1,2}$ and $L^i_{1,2,3}$ for the liquid phase which was obtained during optimization for Ag-Bi, Ag-Sb, Ag-In ,Ag-Ga (Gierlotka & Jendrzejczyk-Handzlik, 2011), Ag-Bi-Pb, Ag-In-Sb and Ag-In-Sn are given in Table 6. Consequently, having these parameters, all thermodynamic properties of the liquid solution were obtained.

Alloy	Parameter [J/mol*atom]
Ag-Bi	$L^0_{Ag,Bi}$ = 6966.59 – 4.41727 * T $L^1_{Ag,Bi}$ = -5880.40 + 1.54912 * T $L^2_{Ag,Bi}$ = -1942.30
Ag-Sb	$L^0_{Ag,Sb}$ = -3619.5 – 8.2962 * T $L^1_{Ag,Sb}$ = -21732.2 + 8.4996 * T $L^2_{Ag,Sb}$ = -6345.2 + 3.2151 * T
Ag-In	$L^0_{Ag,In}$ = -13765.1 – 4.803 * T $L^1_{Ag,In}$ = -11431.5 – 0.031 * T $L^2_{Ag,In}$ = -1950.3 + 1.193 * T
Ag-Ga	$L^0_{Ag,Ga}$ = −19643.7987 + 63.6589 ∗ T − 8.6202∗ T ∗ LN(T) $L^1_{Ag,Ga}$ = −38747.7601 + 140.7162 ∗ T − 16.1115 ∗ T ∗ LN(T) $L^2_{Ag,Ga}$ = −25745.6828 + 140.4553 ∗ T − 17.4166 ∗ T ∗ LN(T)
Ag-Bi-Pb	$L^0_{Ag,Bi,Pb}$ = -94764.84 + 125.336 * T
Ag-In-Sb	$L^0_{Ag,In,Sb}$ = 86 430.422 – 42.845 * T $L^1_{Ag,In,Sb}$ = -13 637.324-7.288 * T $L^2_{Ag,In,Sb}$ = -2752.724 + 4.671 * T
Ag-In-Sn	$L^0_{Ag,In,Sn}$ = 53 189.354 – 3.916 * T $L^1_{Ag,In,Sn}$ = 37 602.644 + 8.536 * T $L^2_{Ag,In,Sn}$ = 1 044.964 – 39.915 * T

Table 6. Binary and ternary parameters for the silver alloys.

5. Conclusion

Electrochemical measurements assure versatile and flexible approach to the investigations of high-temperature systems. Not only thermodynamic properties of solid or liquid phases

can be determined, but also properly design cell can be used as a sensor to monitor concentration changes in either liquid or gaseous phase. Though at present research efforts made on the development of new sensors shifted towards miniaturization and low temperature working conditions, still high- temperature industrial problems with process and quality control as well as environmental protection require continuous monitoring of the behavior of a number of substances. While the main problem with new sensors development is the transfer of the laboratory cell concept into the device operating under industrial conditions, the basic research is still needed to prepare and understand materials which can be used as potential electrolytes. It is our personal point of view that among variety of choices which can be made future progress will be connected with the investigations of three types of stable solid ionic conductors.

5.1 Ceria – based oxygen conducting solid electrolyte

It is known that substitution of cerium ion with the rare earth trivalent ion on the cerium site in CeO_2 lattice enhances conductivity of ceria, with the highest values obtained for Sm_2O_3 (Inaba & Tagawa, 1996) and Gd_2O_3 additions(Sammes & Du, 2005).

The maximum conductivity of the solid solution is observed between 10 and 20 mol % of Sm_2O_3 and Gd_2O_3 addition, and its value reaches $5*10^{-3}$ S/cm at 500 ^{0}C. Apart from the possible application in fuel cells technology (SOFC), this electrolyte may enable thermodynamic measurements at much lower temperature than zirconia does. Its weakness is the response to relatively high oxygen pressure which causes electronic conductivity in this material at high temperature.

5.2 Lanthanum fluoride solid electrolyte

An incredible fast response of the cell with LaF_3 electrolyte to oxygen pressure changes (about 2 min at room temperature) (Yamazoe et al, 1987) makes it very promising material for various sensor construction. Since the only mobile species in lanthanum fluoride are fluoride ions, the mechanism of this rapid response is not completely known (Fergus, 1997).

It was demonstrated by Alcock and Li in 1990, that measurements of the thermodynamic properties of oxides and sulfides performed with fluoride electrolytes are possible also at high-temperature. Since between SrF_2 and LaF_3 solid solution is formed with the highest melting point about 1835 K at the 70 mole% SrF_2- 30 mole % LaF_3 composition , this solid solution was used as a matrix to form so-called composite electrolyte. In this electrolyte a second phase (in this case either oxide or sulfide) was dispersed and appropriate electrochemical cells were assembled. The results demonstrated that this kind of composite can function satisfactorily and the dispersion of sulfides, carbides or nitrides may lead to the fabrication of electrolytes suitable for sulfur, carbon and nitrogen detection.

5.3 Sulfide ionic conductor

Sulfides are usually less stable and more disordered than oxides. Consequently, it is difficult to find sulfide which exhibit entirely ionic conductivity. The most stable sulfides like MgS, CaS, SrS and BaS exhibit NaCl-type structure with ionic bonds, and have high melting point above 2000 K. Thus, they can be considered as potential solid electrolytes. Nakamura and

Gunji (Nakamura & Gunji, 1980) showed that pure CaS is an intrinsic ionic conductor, however it is not a practical material for the solid electrolyte because of its very small conductivity. In turn, magnesium and strontium sulfides have thermodynamic stability and electrical conductivity comparable to CaS, however at high sulfur pressure (between 10^{-7} and 10^{-4} Pa) p-type conduction appears in these materials.

Recently, Nakamura et al in 1984 obtained highly ionic conductor of sulfides by preparing $95CaS–5Na_2S$ solid solution. This material exhibits conductivity about two orders in magnitude higher than any other sulfide, which additionally is independent on sulfur pressure. They also demonstrated that the e.m.f. cell Fe, FeS /$95CaS\text{-}5Na_2S$/ Mn, MnS worked reversibly indicating that ionic transference number is equal to one. It is not certain however, which ion is a predominant charge carrier. Though these experiments may be at present only of laboratory interest , still they may lead to the technique enabling to obtain precise thermodynamic data for sulfide systems. Thus, a lot of new problems wait for those who enter this field. We are convinced that this research area is far from being closed. There is still a lot to be discovered and potential applications are enormous and fascinating. We can only hope that at least to certain extent we'll be able to take part in this developing history, and be a witness of new surprises waiting ahead for us.

6. References

Alcock, C. B. (1968). *Electromotive Force Measurements in High-temperature Systems*. Procedings of a symposium held by the Nuffield Research Group, Imperial College, London, England

Alcock, C. B. & Belford, T. N. (1964). Thermodynamics and solubility of oxygen in liquid matals from e.m.f. measurements involving solid electrolytes. *Transactions of the Faraday*, Vol. 60, pp. 822-835

Alcock, C. B. & Li, B. (1990). A Fluoride-based composite electrolyte; *Solid State Ionics*, Vol. 39, pp. *245-249*

Bednorz, J. G. & Muller, K. A. (1986). Possible high T_c superconductivity in the Ba-La-Cu-O system. *Zeischrift für Physic B- Condensed Matter*, Vol. 64, pp. 189-193

Chang, Y. A., Fitzner, K. & Zhang, M. Z. (1988). The solubility of gases in Liquid Metals and Alloys. *Progress in Materials Science,* Vol. 32, No. 2/3, pp. 98-259, ISSN 0079-6425

Dinsdale, A. T. (1991). SGTE Data for Pure Elements. *CALPHAD*, Vol. 15, pp. 317-425

Fergus, J. W. (1997). The application of solid fluoride electrolytes in chemical sensors; *Sensors and ActuatorsB*, Vol. 42, pp. 119-130.

Fitzner, K. (1990). Gibbs free energy of solid phase $CuEu_2O_4$ and $CuEuO_2$. *Thermochimica Acta*, Vol. 171, pp. 123-130

Fitzner, K., Musbah, O., Hsieh, K. C., Zhang, M. X., Chang, A. (1993). Oxygen potentials and phase equilibria of the quatenary Y-Ba-Cu-O system in the region in the involving the $YBa_2Cu_3O_{7-x}$ phase. *Materials Chemistry and Physics*, Vol. 33, pp. 31-37

Flood, H., Forland, T. & Motzfeld, K. (1952). On the oxygen electrode in molten saltz. *Acta Chemica Scandinavica*, Vol. 6, pp. 257-269

Gąsior, W., Pstruś, J., Moser, Z., Krzyżak, A., Fitzner, K. (2003). Surface tension and thermodynamic properties of liquid Ag-Bi solutions. *Journal of Phase Equilibria,* Vol. 24, pp. 40-49

Gierlotka, W. & Jendrzejczyk-Handzlik, D. (2011). Thermodynamic description of the binary Ag–Ga system. *Journal of Alloys and Compounds*, Vol. 509, pp. 38-42

Goto, K. S. & Pluschkell, W. (1972). *Oxygen Concentration cells in Physics of Electrochemistr*, v 2, Ed. J. Hladzik, Academic Press

Holub, L., Neubert, F. & Sauerwald F. (1935). Die prüfung des massenwirkungsgesetzes bei konzentrierten schmelzflüssigen lösungen durch potentialmessungen. *Zeitschrift für Physikalische Chemie,* Vol. 174, pp. 161-198

Hultgren, R., Desai, P.D., Hankin, D. T., Gleiser, M., Kelly, K. K. (1973). Selected Values of the Thermodynamic Properties of Binary Alloys, American Association for Metals

Inaba, H. & Tagawa, H. (1996). Ceria-based solid electrolytes. *Solid State Ionics*, Vol. 83, pp.1

Jendrzejczyk, D. & Fitzner, K. (2005). Thermodynamic properties of liquid silver–indium alloys determined from e.m.f. measurements. *Thermochimica Acta*, Vol. 433, pp. 66-71

Jendrzejczyk-Handzlik, D,; Gierlotka, W & Fitzner, K. (2006). Thermodynamic properties of liquid silver-indium-antimony alloys determined from e.m.f. measurements. *International Journal of Materials Research*, Vol. 97, pp. 1519-1525

Jendrzejczyk-Handzlik, D., Gierlotka, W. & Fitzner, K. (2008). Thermodynamic properties of liquid silver-indium-tin alloys determined from e.m.f. measurements. *International Journal of Materials Research*, Vol. 99, pp. 1213-1221

Jendrzejczyk-Handzlik, D. & Fitzner, K. (2011). Thermodynamic properties of liquid silver–gallium alloys determined from e.m.f. and calorimetric measurements. *The Journal of Chemical Thermodynamics*, Vol. 43, pp. 392-398

Kiukkola, K. & Wagner, C. (1957). Measurements on galvanic cells involving solid electrolytes. *Journal of the Electrochemical Society*, Vol. 104, pp. 379-387

Kopyto, M. & Fitzner, K. (1996)Gibbs energy of formation of $Cu_2Ln_2O_5$ (*Ln* = Yb, Tm, Er, Ho, Dy) and $CuGd_2O_4$ compounds by the e.m.f. method. *Journal of Materials Science*, Vol. 31, pp. 2797-2800

Kopyto, M. & Fitzner, K. (1997). Gibbs free energy of formation of Ln_2CuBaO_5 compounds determined by the EMF method (*Ln* = Yb, Tm, Er, Ho, Dy and Gd). *Journal of Solid State chemistry*, Vol. 134, pp. 85-90

Kopyto, M. & Fitzner, K. (1999). Gibbs free energy of formation of $LnBa_2Cu_3O_{7-x}$ phases determined by the EMF method (*Ln* = Yb, Tm, Er, Ho, Dy). *Journal of Solid State Chemistry*, Vol. 144, pp. 118-124

Kopyto, M., Kowalik, E. & Fitzner, K. (2003). Gibbs free energy of formation of the Nd_2BaCuO_5 phase determined by the e.m.f. method. *The Journal of Chemical Thermodynamics*, Vol. 35, pp. 773-746

Krzyżak, A., Garzeł, G. & Fitzner, K. (2003). Thermodynamic properties of the liquid Ag-Bi-Pb solutions. *Archives of Metallurgy and Materials*, Vol. 48, No. 4, pp. 371-382

Krzyżak, A. & Fitzner, K. (2004). Thermodynamic properties of liquid silver-antimony alloys determined from emf measurements. *Thermochimica Acta*, Vol. 414, pp. 115-120

Levitskii, V. A. (1978). Nekotoryie Pierspiektivy Primyenieniya Metoda E.D.S. so Ftor-ionnym elektrolitom dlya tiermodinamitsheskovo isslyedovaniya tugoplavkich dvoynych okisnych soyediniyenii. *Vestniki Moskovskovo Universiteta, Seria Khimiya*, Vol. 19, pp. 107-126

Lorentz, R. & Michael, F. (1928). Phyrochemische Daniellketten. *Zeitschrift für Physikalische Chemie,* Vol. 137, pp. 1-17

Muggianu, Y. M., Gambino, M. & Bros, L. P. (1975). Enthalpies of formation of liquid alloys bismuth-gallium tin at 723 K. Choice of an analytical representation of integral and partial excess functions of mixing. *The Journal of Chemical Physics*, Vol. 72, pp. 83-88

Nakamura, H. & Gunji, K. (1980). Ionic conductivity of pure solid calcium sulfide. *Transactions of the Japan Institute of Metals,* Vol. 21, pp. 375-382

Nakamura, H., Ogawa, Y., Gunji, K., Kasahara, A. (1984). Ionic and positive hole conductivities of solid magnesium and strontium sulfides. *Transactions of the Japan Institute of Metals,* Vol. 25, pp. 692-697

Nakamura, H., Maiwa, K. & Iwasaki, S. (2006). Ionic conductivity and Transference number of CaS – Na_2S solid solution. *Shigen-to-Sozai,* Vol. 122 pp. 92-97

Onderka, B., Wypartowicz, J. & Fitzner, K. (1991). Interaction between oxygen and phosphorus in liquid gallium. *Archives of Metallurgy and Materials*, Vol. 36, pp. 5-12

Onderka, B., Kopyto, M. & Fitzner, K. (1999). Gibbs free energy of formation of a solid Sm_2CuBaO_5 phase determined by an e.m.f. method. *The Journal of Chemical Thermodynamics*, Vol. 31, pp. 521-536

Onsager, L. (1931). Reciprocal relations in irreversible processes. *Physical Review*, Vol. 37, pp. 405-426

Przybyło, W. & Fitzner, K. (1996). Gibbs free energy of formation of $Cu_2In_2O_5$ by EMF method. *Archives of Metallurgy and Materials,* Vol. 41, pp. 141-147

Przybyło, W. & Fitzner, K. (1996). Gibbs free energy of formation of the solid phases $Cu_2Y_2O_5$ and $CuYO_2$ determined by the EMF method. *Thermochimica Acta*, Vol. 264, pp. 113-123

Przybyło, W., Onderka, B. & Fitzner, K. (1996). Gibas free energy of formation of $Eu_{1+y}Ba_{2-y}Cu_3O_7$ and related phases in the Eu_2O_3-CiO-BaO system. *Journal of Solid State Chemistry*, Vol. 126, pp. 38-43

Ramanarayanan, T. A. & Rapp, R. A. (1972). The diffusivity and solubility of oxygen in liquid tin and solid silver and the diffisivity of oxygen in solid nickel. *Metallurgical and Material Transaction*, Vol. 3, pp. 3239-3246

Rapp, R. A. & Shores, D. A. (1970). *Solid Electrolyte Galvanic Cells in Physicochemical Measurements in metals Research,* v IV. Ed. R. A. Rapp

Redlich, O. & Kister, A. (1948). Algebraic Representation of Thermodynamic Properties and the Classification of Solutions. *Industrial and Engineering Chemistry*, Vol. 40, pp. 345-348

Sackur, O. (1913). Geschmolzene salze als lösungsmittel. III. Mitteilung: Der dissociationsgrad gelöster Salze. *Zeitschrift für Physikalische Chemie,* Vol. 83, pp. 297-314

Salstrom, E. J. & Hildebrand, J. H. (1930). The thermodynamic properties of molten solutions of lead chloride in lead bromide. *Journal of the American Chemical Society,* Vol. 52, pp. 4641-4649

Salstrom, E. J. & Hildebrand, J. H. (1930). The thermodynamic properties of molten solutions of lithium bromide in silver bromide. *Journal of the American Chemical Society,* Vol. 52, pp. 4650-4655

Salstrom, E. J. (1933). The free energy of reactions Involving the fused chlorides and bromides of lead, zinc and silver. *Journal of the American Chemical Society,* Vol. 55, pp. 2426-2428

Seltz, H. (1935). Thermodynamics of solid solutions. II. Deviations from Roult't law. *Journal of the American Chemical Society,* Vol. 57 (March), pp. 391-395

Sammes, N. & Du, Y. (2005). *Intermediate-temperature SOFC Electrolytes, in Fuel Cell Technologies State and Perspectives,* Ed. N. Sammes, Springer pp.19-34

Spencer, P. J. & Kubaschewski, O. (1978). A thermodynamic assessment of the iron-oxygen system. *Calphad*, Vol. 2, pp. 147-167

Subbarao, E. C. (1980). *Electrolytes and Their Applications*. Plenum Press, New York, ISBN 3-306-40389-7

Tammann, Von G. (1924). Die Spannungen der Daniellketten mit flüssigen chloriden und die spannungsreihe der metalle in flüssigen chloriden. *Zeitschrift für Anorganische und Allgemeine Chemie*, Vol. 133, pp. 267-276

Taylor, N. W.(1923). The activities of zinc, cadmium, tin, lead and bismuth in their binary liquid mixtures. *Journal of the American Chemical Society*, Vol. 45, pp. 2865-2890

Turkdogan, E. T. (1980). *Physical Chemistry of High Temperature Technology*, Academic Press New York, ISBN 0-12-704650-X

Wagner, C. (1933). Beitrag zur Theorie des Anlaufvorgangs. *Zeitschrift für Physikalische Chemie-Abteilung B-Chemie der Elementarprozesse Aufbau der Materie*, Vol. 27, pp. 25–41

Wagner, C. (1936). Beitrag zur Theorie des Anlaufvorgangs II. *Zeitschrift für Physikalische Chemie*, Vol. 14, pp. 447-462

Wu, M. K., Ashburn, J. R., Torng, C. J., Hor, P. H., Meng, M. L., Gao, L., Huang, Z. J., Wang, Y. Q., Chu, C. W. (1987). Superconductivity at 93 K in a new mixed-phase Y-Ba-Cu O compound system at ambient pressure. *Physical Review Letters* Vol. 58, pp. 908-910

Wypartowicz, J. & Fitzner, K. (1987). Activity of oxygen in dilute solutions of arsenide in liquid phase with and without gallium additions. *Journal of the Less-Common Metals*, Vol. 128, pp. 91-99

Wypartowicz, J. & Fitzner, K. (1988). Activity of oxygen in dilute solution of arsenic in liquid galium. *Journal of the Less-Common Metals*, Vol. 138, pp. 289-301

Wypartowicz, J & Fitzner, K. (1990). Activity of oxygen in a dilute solution of phosphorus in liquid indium. *Journal of the Less-Common Metals.* Vol. 159, pp. 35-42

Yamazoe, N., Hisamoto, J. & Miura, N. (1987). Potentiometric solid-state oxygen sensor using Lanthanum Fluoride operative at room temperature, *Sensors and Actuators*, Vol. *12*, pp. 415-423.

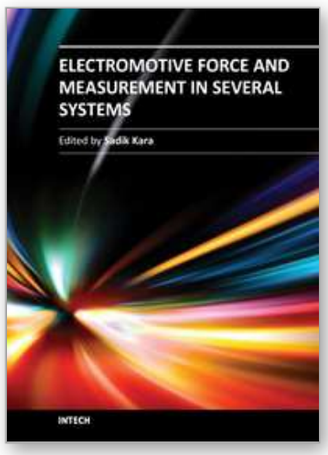

Electromotive Force and Measurement in Several Systems

Edited by Prof. Sadik Kara

ISBN 978-953-307-728-4
Hard cover, 174 pages
Publisher InTech
Published online 21, November, 2011
Published in print edition November, 2011

This book is devoted to different sides of Electromotive Force theory and its applications in Engineering science and Industry. The covered topics include the Quantum Theory of Thermoelectric Power (Seebeck Coefficient), Electromotive forces in solar energy and photocatalysis (photo electromotive forces), Electromotive Force in Electrochemical Modification of Mudstone, The EMF method with solid-state electrolyte in the thermodynamic investigation of ternary copper and silver chalcogenides, Electromotive Force Measurements and Thermodynamic Modelling of Electrolyte in Mixed Solvents, Application of Electromotive Force Measurement in Nuclear Systems Using Lead Alloys, Electromotive Force Measurements in High-Temperature Systems and finally, Resonance Analysis of Induced EMF on Coils.

INTECH
open science | open minds

InTech Europe
University Campus STeP Ri
Slavka Krautzeka 83/A
51000 Rijeka, Croatia
Phone: +385 (51) 770 447
Fax: +385 (51) 686 166
www.intechopen.com

InTech China
Unit 405, Office Block, Hotel Equatorial Shanghai
No.65, Yan An Road (West), Shanghai, 200040, China
中国上海市延安西路65号上海国际贵都大饭店办公楼405单元
Phone: +86-21-62489820
Fax: +86-21-62489821

IntechOpen